A Hybrid Expert System for Individualized Quantification of Electrical Status Epilepticus During Sleep Using Biogeography-Based Optimization

Wei Zhou, Xian Zhao, Xinhua Wang, Yuanfeng Zhou, Yalin Wang, Long Meng, Jiahao Fan, Ning Shen, Shuizhen Zhou, Wei Chen, *Senior Member, IEEE*, and Chen Chen

***Abstract*— Electrical status epilepticus during sleep (ESES) is an epileptic encephalopathy in children with complex clinical manifestations. It is accompanied by specific electroencephalography (EEG) patterns of continuous spike and slow-waves. Quantifying such EEG patterns is critical to the diagnosis of ESES. While most of the existing automatic ESES quantification systems ignore the morphological variations of the signal as well as the individual variability among subjects. To address these issues, this paper presents a hybrid expert system that dedicates to mimicking the decision-making process of clinicians in ESES quantification by taking the morphological variations, individual variability, and medical knowledge into consideration. The proposed hybrid system not only offers a general scheme that could propel a semi-auto morphology analysis-based expert decision model to a fully automated ESES quantification with biogeography-based optimization (BBO), but also proposes a more precise individualized quantification system to involve the personalized characteristics by adopting an individualized parameters-selection framework. The feasibility and reliability of the proposed method are evaluated on a clinical dataset collected from twenty subjects at Children's Hospital of Fudan University, Shanghai, China. The estimation error for the individualized quantitative descriptor ESES is 0-4.32% and the average estimation error is 0.95% for all subjects. Experimental results show the presented system outperforms existing works and the individualized system significantly improves the performance of ESES quantification. The favorable results indicate that the proposed hybrid expert system for automatic ESES quantification is promising to support the diagnosis of ESES.**

***Index Terms*— Biogeography-based optimization, electroencephalography, electrical status epilepticus during sleep.**

I. Introduction

ELECTRICAL status epilepticus during sleep (ESES) is a syndrome of epileptic encephalopathy with onset either in infancy or childhood [1], [2]. It is one of the rare forms of epilepsy-related to the decline in cognitive, behavioral, and psychomotor abilities, and it is also associated with complex etiologies such as structural brain abnormalities, genetic abnormalities, etc. Persistent ESES can lead to children's abnormal development, including cognitive impairment, behavioral disturbance, and language function decay [3], [4]. Therefore, accurate diagnosis and active intervention of ESES as early as possible are significant to improve the prognosis of ESES. However, children with ESES often show various and complex clinical manifestations, adding difficulty to the early diagnosis of the disease. Electroencephalography (EEG), as the gold standard in the diagnosis of epilepsy, also plays an important role in the diagnosis of ESES [5]. The patients with ESES, accompanied by strong activation of epileptiform activity during slow sleep, present the particular EEG patterns of continuous spike and slow-wave abnormalities [6]. Such signal patterns characterize the typical ESES patterns. Evaluating EEG with the quantitative descriptor of ESES patterns plays a key role in diagnosing and treating patients [5], [7]. Clinically, the quantitative descriptor is usually obtained through visual inspecting EEG recordings over time and marking ESES patterns by an experienced expert. This quantification process is time-consuming and makes clinicians weary. Moreover, manual scoring results can be variable from different observers.

Manuscript received 24 November 2021; revised 8 April 2022; accepted 13 June 2022. Date of publication 28 June 2022; date of current version 19 July 2022. This work was supported in part by the Shanghai Municipal Science and Technology International Research and Development Collaboration Project under Grant 20510710500, in part by the National Natural Science Foundation of China under Grant 62001118, and in part by the Shanghai Committee of Science and Technology under Grant 20S31903900. *(Corresponding authors: Chen Chen; Shuizhen Zhou; Wei Chen.)*

This work involved human subjects or animals in its research. Approval of all ethical and experimental procedures and protocols was granted by the Hospital Ethical Committee under Approval No. (2020) 173.

Wei Zhou, Xian Zhao, Long Meng, and Ning Shen are with the Center for Intelligent Medical Electronics (CIME), School of Information Science and Engineering, Fudan University, Shanghai 200437, China (e-mail: wzhou19@fudan.edu.cn; xzhao17@fudan.edu.cn; 18110720062@fudan.edu.cn; nshen20@fudan.edu.cn).

Xinhua Wang, Yuanfeng Zhou, and Shuizhen Zhou are with the Department of Neurology, Children's Hospital of Fudan University, Shanghai 201102, China (e-mail: xiner.1211@163.com; yuanfengzhou@fudan.edu.cn; szzhou@shmu.edu.cn).

Yalin Wang, Jiahao Fan, and Chen Chen are with the Human Phenome Institute, Fudan University, Shanghai 200437, China (e-mail: 19110720062@fudan.edu.cn; 18110720059@fudan.edu.cn; chenchen_fdfudan.edu.cn).

Wei Chen is with the Center for Intelligent Medical Electronics (CIME), School of Information Science and Engineering, and the Human Phenome Institute, Fudan University, Shanghai 200437, China (e-mail: w_chen@fudan.edu.cn).

Digital Object Identifier 10.1109/TNSRE.2022.3186942

Therefore, developing automatic methods for quantifying EEG pattern related to ESES is essential to relieve the burden of doctors and contribute to the early diagnosis and treatment of children with ESES.

Quantifying ESES-related EEG aims to provide the quantitative descriptor of ESES patterns, which expresses the percentage of ESES activity during sleep to diagnose patients. It requires the methods to recognize ESES patterns in sleep EEG and evaluate them with the quantitative descriptor. As ESES patterns are characterized by continuous spike and slow-waves abnormalities, some investigators try to find ESES patterns through detecting spikes, which are parts of characteristic waves of ESES patterns. The automatic ESES quantification methods can be roughly classified into machine learning-based approach and knowledge-based approach. Most of machine learning-based techniques can achieve favorable performance [8]–[13]. For example, to accomplish the automated classification of epileptic seizures, Supriya *et al.* developed a graph theory-based innovative framework [14]. Zarei *et al.* proposed a new scheme based on principal component analysis and machine learning techniques [15]. However, it also requires big volumes of data to explore and build the decision-making model. As an epileptic encephalopathy, the features of ESES are rather different from epileptic seizures. Besides, due to the scarcity of cases, the data belonging to ESES is much smaller. Thus, we proposed a hybrid expert system integrating biogeography-based optimization method instead of simply applying machine learning methods. As for the knowledge-based approach, it can offer a straightforward and explainable solution for ESES quantification. To illustrate, Nonclercq *et al.* [16] proposed an automatic spike detection method based on template matching to apply ESES quantification. Favorable detection results can be obtained when the shape of the chosen template is similar to the contour of the spike portion of ESES patterns. However, with the evolution of ESES activity [17], its characteristic wave can vary in amplitude and duration, which would increase false detections. Considering variable spikes in EEG, Nonclercq *et al.* [18] improved the algorithm using clustering to include various shapes of spike waves. The detection performance was elevated, but the presented algorithm still largely relied upon the pre-selected templates. Although these works suggested that the quantification of ESES patterns could be achieved by detecting spikes, all of them only identified the spike waves coming from the simple spike and slow waves. They ignored the interlaced overlapped spike and slow waves. This type of ESES waveform is more complex and frequently occurs as ESES activity evolves. Moreover, in terms of assessing the duration of ESES pattern, these spike detection-based methods led to a significant bias due to the lack of slow-wave abnormalities detection. These defects also imply that many other approaches designed for spike detection are not appropriate for the automatic quantification of ESES activity [19], [20].

As ESES is one of the rare epilepsies, the related and well-labeled data are challenging and expensive to obtain, in which case a suitable morphology analysis-based expert decision model (MA-EDM) can be a better solution to identify and quantify ESES patterns [21]. Results from our previous work have demonstrated their great potential for the application of the quantification of ESES patterns. Nevertheless, this existing knowledge-based approach still has some issues that need to be resolved. First, morphological filtering-based feature detectors were designed to distinguish features from time series, whose parameters severely affect the identification accuracy of ESES patterns. Manual regulation of these parameters was adopted by the approach, which ignores the morphological variation of signals. Second, feature extraction operation was used to localize and extract features, where the horizon can influence the duration estimation of ESES patterns. The same and empirical horizon was used by the approach for all features, which overlooked the differences among features. Finally, the approach did not consider individual characteristics. To improve this knowledge-based approach for automatic quantification of ESES patterns, morphological variation of signals and different features should be considered in the decision model.

In this paper, a hybrid expert system integrating biogeography-based optimization techniques into the morphology analysis-based expert model for quantifying ESES is proposed. It dedicates to mimicking the decision-making process of clinicians in ESES quantification by considering the personalized characteristics and medical knowledge. Firstly, a parameter selection scheme on basis of biogeography-based optimization algorithm to propel a semi-auto MA-EDM model to a fully automated ESES quantification model is devised. Secondly, based on the automatic scheme, an individualized ESES quantification system that takes account of personalized characteristics is proposed. Finally, the impact of the amount of prior knowledge on the individualized ESES quantification is explored and the minimum percentage of individual data for generating the appropriate feature detector and extraction operation parameters is provided. The main contributions of this paper can be summarized as follows.

1) The proposed scheme offers an effective solution for automatically adjusting the feature detector and extraction operation parameters.
2) By involving little prior knowledge, the individualized ESES quantification system could achieve superior performance as compared with the automatic scheme.
3) We explored the performance that can be achieved with as small amount of training data as possible.

The proposed system allows an automated setting-up and adjustment of feature detector and extraction operation by considering not only signal morphology but also personalized characteristics. Therefore, the proposed hybrid expert system is expected to significantly improve the performance of ESES quantification.

II. Method

In this section, our previous work is briefly introduced and then an automatic ESES quantification scheme and an individualized system based on biogeography-based optimization are proposed.

A. EEG Quantification Scheme Using Expert Knowledge and Morphology Analysis

A brief description of MA-EDM is presented below, more details can be found in our previous work [21].

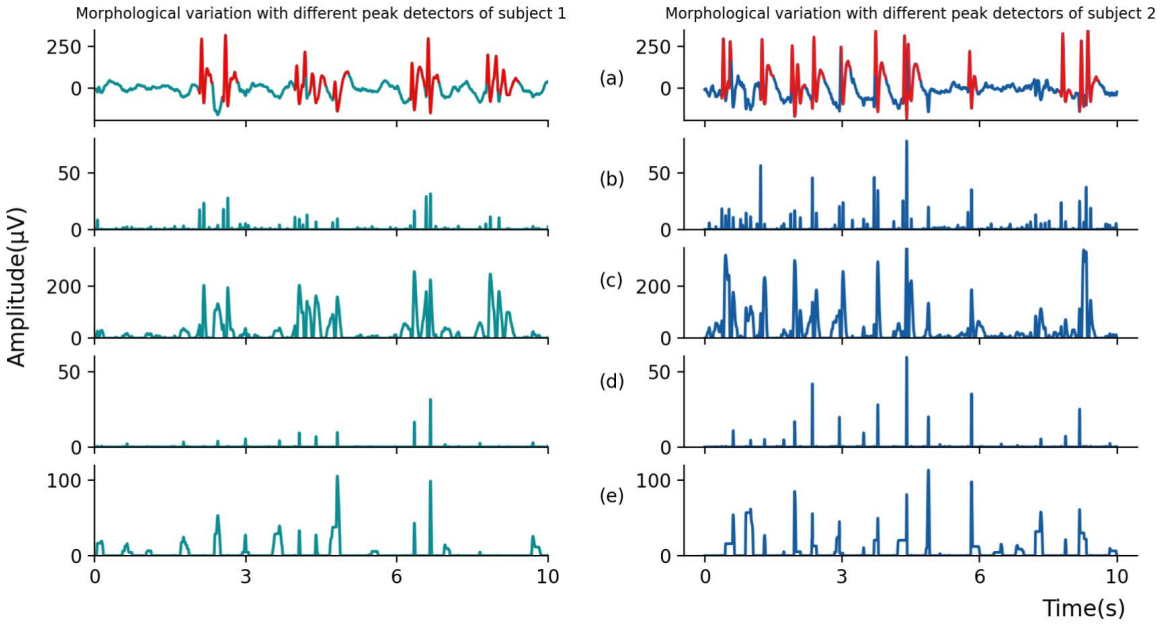

Fig. 1. Two examples of EEG signals and the corresponding results obtained with different peak detectors. The left and right sides drawn using different colors are the results of two subjects respectively. Different values of length $W_{1,2}$ are predefined for the detector. The height of structuring elements h_k is the same value of 3 as in [21]. (a) Original EEG signals, where actual spike and slow-waves labeled by the expert are plotted in red color. (b) The signal from the peak detector with W_1=3 and W_2=3. (c) The signal from the peak detector with W_1=3 and W_2=30. (d) The signal from the peak detector with W_1=30 and W_2=3. (e) The signal from the peak detector with W_1=30 and W_2=30.

1) Data Preprocess: Raw EEG signals were filtered to remove artifacts. As ESES is a typical EEG waveform during sleep. Only sleep EEG characteristic is considered in this paper. According to the American Academy of Sleep Medicine (AASM) guidelines [22], the recommended filter setting for EEG derivations is 0.3-35 Hz. In this paper, in conjunction with AASM and the clinician's recommendation, we used a bandpass filter from 0.5 to 40 Hz and 400μV for noise elimination.

2) Morphological Feature Extraction: The spike and slow-waves abnormalities in ESES activity can be identified using morphological features, namely positive peaks, negative pits, and corresponding temporal sequences of them. Positive peaks or negative pits are firstly discriminated from time series by performing peak/pit detector, followed by the feature extraction operation to extract them from signals. Feature detectors constructed by morphological filters (MF) are designed and performed to the pre-processed signal. They can separate morphological features from signals meanwhile restrain the interference from background waves [23], [24]. For the pre-processed signal EEG signal $f(n)$ of length N, the result by performing peak detector (PKD) and pit detector (PTD) on f(n) can be expressed using 1 and 2, respectively.

$$p_k(n) = PKD[f(n)] = (f \circ g_1)(n) - [(f \circ g_1) \bullet g_2)](n) \tag{1}$$

$$p_t(n) = PTD[f(n)] = (f \bullet g_1)(n) - [(f \bullet g_1) \circ g_2)](n) \tag{2}$$

where $\circ$ and $\bullet$ denote opening operation and closing operation, respectively. $g_i(n), i = 1, 2, 3, 4$ is the same dome-like structuring element but has different widths W_i as follows, whose width or length $(2 * W_i)$ mainly relies upon the length of signal features to be detected.

$$g_i(n) = \begin{cases} h \times [1 - exp(-n)], & for\ n = 0, 1, \ldots, W_i \\ g(2W_i - n), & for\ n = W_i + 1, \ldots, 2W_i \end{cases} \tag{3}$$

Feature extraction operation is employed to all obtained results p. The beginning and ending points of these features are also estimated, which provide important clues for the latter identification of spike and slow-waves. Using (4) firstly transforms the features (peak/pit) in the obtained result p into bipolar oscillating impulses (positive-negative/ negative-positive) in the output c. Then, for each bipolar oscillating impulse, the first local extreme point (maximum/minimum) on its left is detected as the beginning of the features (peak/pit); the extreme point (minimum/maximum) on its left on its right is detected as the end of the features (peak/pit).

$$c(n) = FC[p(n)] = \sum_{m=0,\ldots,r-1} p(n+m) - p(n), \quad for\ n = 1, 2, \ldots, L - r + 1 \tag{4}$$

where $FC[\cdot]$ represents the functional calculus that summates the differences of input signal p (namely p_k, p_t) in a forward horizon r. The c represents the output data.

3) Spike and Slow-Waves Identification: The identification of ESES patterns is performed by judging spike and slow-waves abnormalities from extracted features. For identifying multiple types of spike and slow-waves, the rules inspired by medical knowledge and signal morphology are used to search different complex structures of spike and slow-waves. Those extracted features will be combined and judged as candidates for the spike and slow-wave preliminarily. The recognition is

performed by comparing each candidate with a generalized amplitude criterion, which is taken as the baseline that is commonly used during expert scoring.

$$S^* = \eta(S, Th_l, Th_u) = \begin{cases} f(t_s, t_e), & condition \\ Null, & else \end{cases} \quad (5)$$

where S^* denotes the identified spike and slow-wave. $S = f(t_1, t_2)$ represents the individual candidate whose onset and offset are t_1 and t_2 respectively. Th_u and Th_l represent the amplitude range of non-event waveforms. They can be computed from the histogram of the extreme points in non-event waveforms over the collected data. Condition means that $S_{t=t_e} \geq Th_u$ and $Th_l < S_{t_e \geq t} < Th_u$.

4) Quantitative Measure of ESES Patterns: The quantification of EEG related to ESES is achieved by evaluating spike and slow-waves with the key quantitative parameter, namely the spike-wave index (SWI). Following the guidelines in ESES diagnosis, it can be computed as follows.

$$SWI = \left(\frac{\sum_{j=1}^{K} d_j}{Duration}\right) * 100. \quad (6)$$

where d_j is the estimated duration of the j_{th} spike and slow-wave. K is the number of the detected spike and slow-waves. Duration denotes the non-rapid eye movement sleep (NREM) duration of the record.

5) Limitations of MA-EDM: In the existing work, the parameterized feature detectors were performed manually by authors. However, manually predefined parameters ignore the morphological variation of signals. The morphological features may not be discriminated effectively from time series by the detectors. Fig. 1 displays the corresponding results of EEG signals of two subjects by setting up the peak detector with different regulations. The features are not only related to the parameters of the detector but also related to variances of individuals. Manually predefined values of lengths may not obtain effective features of ESES patterns, and the height of the structuring element used could also affect system performance. The influence of using different heights for peak/pit detector had been explored and shown in our previous work [21]. Moreover, the same and empirical horizon is used by the system MA-EDM for all features, which overlooks the differences between peaks and pits as well as the variation between individuals.

To address these limitations, the following part of the paper presents a solution by constructing a new framework based on hybrid techniques. The signal morphology and different features are considered by the hybrid system employing different parameterized feature detectors and extraction operations for positive peak and negative pit, respectively. It integrates biogeography-based optimization into the decision model to generate and select optimal parameters automatically for them.

B. Proposed Automatic ESES Quantification Scheme Using Biogeography-Based Optimization

Compared with the previous solution, the proposed method integrates the Biogeography-based optimization (BBO) algorithm in the Morphological feature extraction to further improve the performance. BBO is similar to other heuristic optimization algorithms, such as genetic algorithms (GA) [25], particle swarm optimization (PSO) [26], etc. Compared with other algorithms, BBO is able to calculate the corresponding mutation rate according to the number of populations accommodated in the habitat and perform mutation operations on the habitat, which makes the algorithm have a strong adaptive capability. Thus, BBO has the ability to explore solutions quickly and can cross the local optimum. Next, we will briefly introduce the BBO algorithm and our experimental steps.

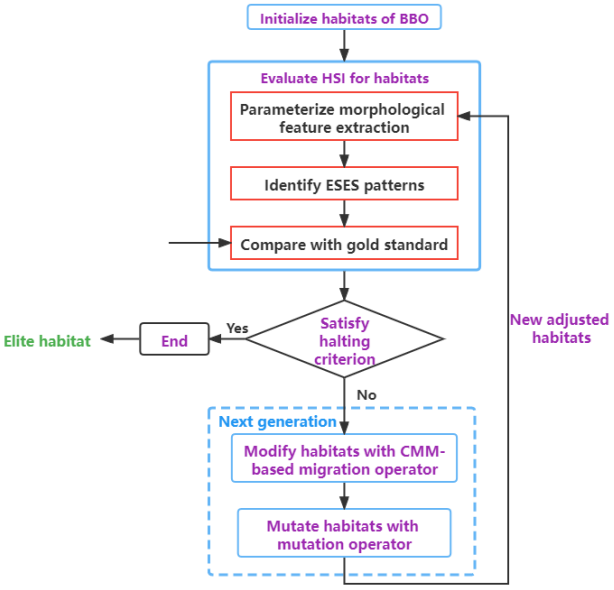

Fig. 2. Flowchart of CMM-BBO-based automatic parameter selection by mapping the identification procedure of ESES patterns into BBO.

In recent years, the exploration of biogeography has been drawing great attention [27]–[32]. BBO was first proposed by Simon [33]. It is a new evolutionary algorithm based on biogeography that is developed to tackle global optimization problems. To measure the stability of habitat, the habitat suitability index (HSI) is used as an indicator. Suitability index variables (SIVs) are independent variables to compute HSI [30]. Many BBO variants have been developed, such as BBO based on new migration or mutation operators [34], [35], BBO hybrid with other evolutionary algorithms [36], [37], and BBO based on multiple populations or local topologies [38]. Chen *et al.* [39] proposed the migration operator based on covariance matrix (CMM) to reduce its reliance on the coordinate system.

In this study, we employed the BBO with CMM-based migration operator, which allows habitats to share their impactful information more efficiently. Following we will explain in detail the optimization of system parameters based on CMM-BBO. It not only offers an automatically parameters adjusting solution but also provides a general scheme for parameter setting-up. As shown in Fig. 2, the automatic parameter selection (APS) mainly consists of the following steps:

1) Initialization of Habitats: We initialize the maximum migration rates E and I for migration operators, the maximum mutation rate m_{max} for mutation operator. The population

consists of NP habitats H_i^G, $i = 1, 2, \ldots, NP$, where G denotes the generation count. Each habitat $H_i^G = (X_{i,1}^G, X_{i,2}^G, \ldots, X_{i,8}^G)$ is represented by an eight-dimensional real system parameter vector. The parameter vector is $[W_{1,2,3,4}, h_k, r_k, h_t, r_t]$, which are regarded as SIVs of the habitat. The individual is initialized as follows.

$$X_{i,d}^G = L_d + rand(0, 1) \times (U_d - L_d). \tag{7}$$

where $i = 1, 2, \ldots, NP$, which denotes the i_{th} individual habitat. U_d and L_d denote the upper bound and lower bound of d_{th} parameter of the system parameter, where $d = 1, 2, \ldots, 8$.

2) Evaluating HSI for Each Habitat: The HSI of habitat is assessed with the objective function of the decision model. In our presented scheme, the F1 score of system performance is taken as the HSI of each habitat in BBO. The F1 score which measures detection performance is calculated by comparing detections with the actual events marked by expert.

3) Modifying Habitats With CMM-Based Migration Operator: For a habitat H_i^G, its immigration rate λ_i is used to probabilistically decide whether to adjust each parameter in that solution. Immigration rate λ_i and emigration rate μ_i can be calculated as follows.

$$\lambda_i = I \times (1 - s/n). \tag{8}$$

$$\mu_i = E \times (s/n). \tag{9}$$

where s is the order index of the individual habitat H_i in H after sorting, which is taken as its species account in the present application. The value of s ranges from 1 to n, where $s = 1$ represents the worst individual while $s = n$ represents the best. n denotes the largest species account, which could be set as $n = NP$.

To minimize the interference of the habitat information sharing, the original coordinate system would be rotated to an eigenvector-based system by the CMM-based migration operator, which is mathematically described in [39].

$$Cov(H^G) = Q_H \Lambda_H Q_H^T. \tag{10}$$

$$eigH_i^G = H_i^G \times Q_H eigH_i^G = (eigX_{i,1}^G, eigX_{i,2}^G, \ldots, X_{i,8}^G). \tag{11}$$

$$H_i^{G+1} = eigH_i^{G+1} \times Q_H^T \tag{12}$$

where Q_H is the $D \times D$ matrix that has the eigenvector of $Cov(H^G)$ as its i_{th} column. Λ_H is the diagonal matrix that has the corresponding eigenvalues as its diagonal entries. $eigH_i^G$ is the rotated solution, $eigX_{i,d}^G$ is the rotated parameter in the eigenvector-based coordinate system, and $i = 1, 2, \ldots .NP$.

4) Mutating the Population With the Mutation Operator: Each habitat has an associated species count probability P_i computed from λ_i and μ_i. A habitat with medium HSI is the most probable solution to the problem. A habitat with very high or low HSI is likely to mutate to a different solution. The mutation operator replaces its SIV with a new random value. Each habitat has a mutation rate m_i measured as follows.

$$m_i = m_{max} \times (\frac{1 - P_i}{P_{max}}) \tag{13}$$

where m_{max} is a control parameter defined by the user, and P_{max} is the probability that the habitat has the most species.

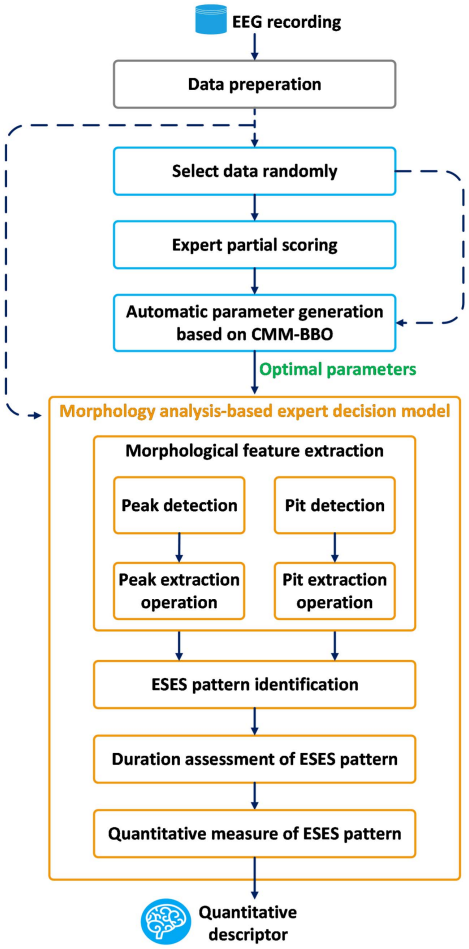

Fig. 3. Scheme of biogeography-based optimization tuned hybrid expert system for individualized quantification.

5) Halting Criterion: The steps above will stop till the halting criterion is satisfied or the maximum number of iterations is reached. The maximum iteration number of objective function evaluations is defined in the experimental setup section. The halting criterion in our scheme is the HSI of 1.0, which corresponds to the F1 score of the decision model. The HSI of each new adjusted habitat will be evaluated and the elite habitat to update the best solutions will be selected.

C. Proposed Individualized Quantification System

The whole process is shown in Fig. 3. To accommodate the variability of individual characteristics, the algorithm is executed separately for different subjects. In the pre-processing and data selection, we read raw EEG signals and reduce the interference from artifacts to signals in the recording. Mapping the identification procedure of ESES patterns into BBO, potential solutions are generated by performing CMM-BBO algorithm on partial EEG data. After comparing their performance with expert scoring, these solutions would be modified using migration and mutation operators till the best solution is searched. As such, the optimal parameters can be generated by adjusting the parameterized operations to the selected signals using CMM-BBO algorithm. By presenting the obtained optimal parameters into the morphology analysis-based expert

decision model, the morphological feature extraction is automatically set up with these parameters. For different features, diverse feature detectors and extraction operations are employed for their extraction. They can be adjusted to the signals by using the obtained parameters. Hence, we can obtain a tuned decision model and apply it to the remaining EEG data to obtain final quantitative results for ESES.

In the presented individualized system, the biogeography-based optimization algorithm is embedded in the decision model for computing system parameters. Meanwhile, the decision model is fused inside the biogeography-based optimization algorithm for evaluating the performance of these parameters. Through this hybrid scheme, the decision model is tuned by the biogeography-based optimization algorithm.

III. Results

A. Data Collection

The data used for this research was obtained from the Children's Hospital of Fudan University, Shanghai, China. A total of 20 children with ESES syndrome (12 males and 8 females) aged from 3 to 14 years old were involved. The data collection was approved by the hospital ethical committee (approval No. (2020) 173). Informed consent was obtained from the parents or legal guardians of each subject before their participation. The data were collected when the subject was in the time of medical examinations. The surface EEG signals at rest were recorded using the Nicolet EEG device which includes the channels from the 10-20 international electrode placement system. The recording lasted 3 hours on average to guarantee a complete sleep cycle of EEG signals. All EEG recordings were digitized at a sampling rate of 500 Hz and stored in the files of EDF format. To evaluate the presented hybrid expert system, the data collected for this research is divided into two sub-datasets. The first dataset includes 4 subjects (2 males and 2 females) aged from 4 to 11 years old. 40 short excerpts (10 excerpts from each subject) that contain the abundance of ESES discharges during sleep were selected and analyzed by the expert. The second dataset includes all long-term recordings from 20 subjects (12 males and 8 females) aged from 3 to 14 years old for final evaluation. Each recording ranges from 179.1 to 195.6 min. The first dataset is used to quantitatively assess the spike and slow waves and to validate the feasibility of the proposed system. The second dataset is used for the final SWI evaluation. While it is worth mentioning that the second dataset contains the whole long-term EEG recordings of these 4 patients, while the first dataset only consists of 40 short excerpts from these 4 patients.

B. Performance Evaluation

The first dataset is adopted to test the feasibility of the presented system by fully assessing the detailed information of spike and slow-wave abnormalities. After that, the system parameters can be generated and tuned to the data related to ESES. We compare detections with events by one-to-one matching. During the matching procedure, two events are compared by employing Intersection over Union (IoU), which has been commonly utilized to quantify the overlap between two events in detection tasks [40]–[43]. An overlap threshold value of a = 0.4 is used, which is stricter than the values of these works [31], [33]. The second dataset is applied to further validate the reliability of the presented system, and the experimental results of the existing methods are compared.

In the experiment on the first dataset, taking the expert as the gold standard, the SWI error and F1 score are computed to evaluate the performance. In addition, we use precise (Pre.), sensitivity (Sens.), and false discovery rate (FDR) to measure the ability of the model for recognizing ESES patterns. Moreover, the assessment of the duration and the quantitative parameter of ESES patterns are involved in the process of quantification. In the experiment on the second dataset, the expert scores the data during sleep by calculating the quantitative descriptor SWI. Different methods are employed on the same dataset, and the SWI results given by the expert and the algorithm are compared.

C. Experimental Setup

For CMM-BBO, several reasonable values, which are suggested in the application of BBO algorithm [39], are adopted to set the following control parameters for the current implementation: population size $NP = 100$, mutation probability $m_{max} = 0.005$, emigration rate E and immigration rate I for habitat = 1, the control parameter of CMM-based migration operator $P_e = 0.5$, elitism parameter $p = 1$, and maximum number of objective function evaluations = 15000. For the morphology analysis-based expert decision model, the bidirectional amplitude threshold $Th_u = 71$ and $Th_l = -25$ is taken, which follows the convention employed for ESES analysis [21]. The presented hybrid expert system is implemented and evaluated in MATLAB R2019a.

To evaluate the feasibility of the presented system, we conducted our experiments over 20 independent runs by applying the system on the first dataset. For each run, 10%, 20%, 50%, 80% of the data were randomly selected as the training set used by the CMM-BBO model for computing optimal parameters, and the remaining data were used for testing the overall quantification system. We have conducted experiments separately for individuals and for group to explore the personalized performance of the proposed system. The minimum training data ratio that achieves considerable accuracy can be obtained through the experiments. Moreover, a comprehensive experiment for the application of ESES evaluation is performed by complementing the proposed system on the second dataset.

D. Experimental Results on the First Dataset

We tested the presented system by implementing it to the excerpts from 4 subjects, which contain the abundance of ESES discharges during sleep. For the presented system running on an Intel Core i5 CPU 3.40 GHz, the average time taken for each run was 69689s. The average time for each iteration was 464.60s. The average convergence time for each run was 27875.71s. The average time taken to evaluate the objective function was 4.65s.

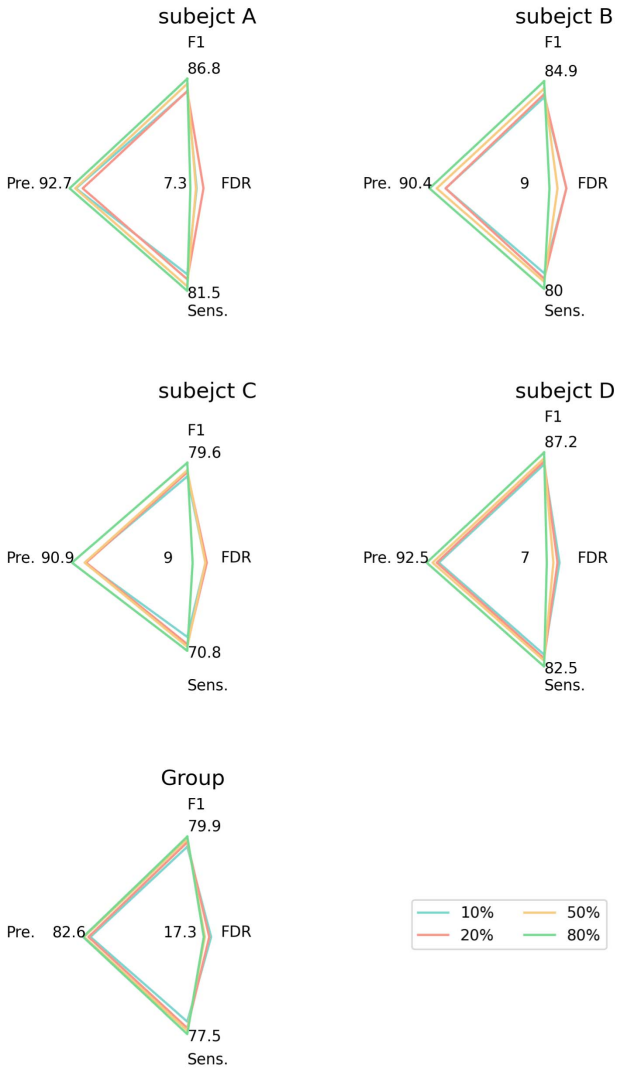

Fig. 4. Results of the individualized and generalized system using different percentages of the training data. Group represents four subjects to train together with the generalized system.

Fig. 4 showed the detection performance of the presented hybrid expert system. Compare with the generalized system, the individualized system trained on individual data obtained better performance. The results for subject C are relatively worse, while the performance of all the other three subjects is considerably higher. Comparing the results of different percentages of training data, it is obvious that the performance of the algorithm increases as the training data increases. The trend is more explicit on individualized system than generalized system. For all subjects, the proposed system achieved the F1 score of almost 0.7 using 10% of the data. When the amount of training data increased to 80%, F1 score increased to more than 0.8. The best detection performance for individuals was obtained on subject D with F1 score of 0.87 using 80% of the data. It showed acceptable performance using fewer data, and superior performance using more data. The overall performances of the algorithm from Fig. 4 demonstrated that the presented individualized hybrid expert system significantly improves the performance of ESES quantification in comparison with the generalized scheme.

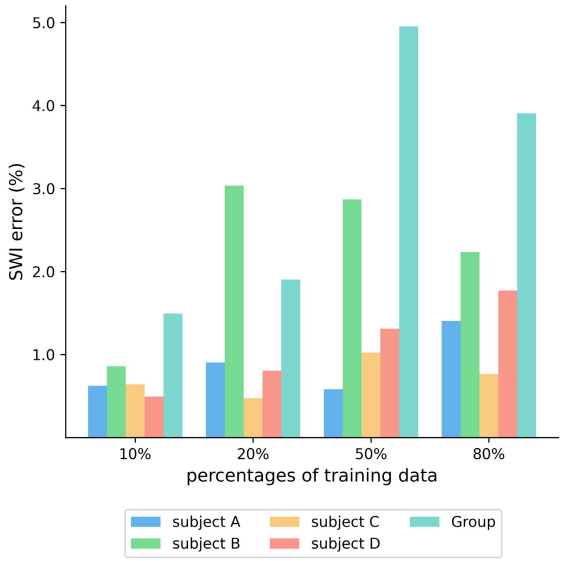

Fig. 5. SWI error obtained by the individualized and generalized system. Results of four subjects training using different percentages (10%, 20%, 50%, 80%) of the data.

Fig. 5 shows the SWI errors for different subjects. It also demonstrates that the presented individualized system outperforms the generalized scheme.However, as the training data increased, the system obtained worse SWI estimation in several subjects. On the one hand, CMM-BBO model regarded F1 score as the target, which leads to the recognition area deviating beyond the actual area, thereby increasing the SWI error. On the other hand, although the SWI error fluctuated within a certain range, the algorithm can still achieve good performance. In estimating the quantitative descriptor SWI, the system enhanced the effectiveness in individual experiments. The SWI error of the presented system was 1.49% for the group of subjects. It had errors within 1% for different subjects. For the SWI evaluation, no significant difference between the results obtained from training with different ratio data was found ($p > 0.05$). Comprehensively considering the amount of data used, the recognition accuracy and the SWI estimation error of the system, 10% can be considered as the appropriate percentage of the data for training in determining the feature detector and extraction operation parameters.

E. Experimental Results on the Second Dataset

To further validate the presented system, we applied the individualized system with the 10% of EEG recordings from 20 subjects with ESES syndrome for evaluating SWI. As shown in Table I, the SWI errors of twenty subjects between individualized system and expert were from 0 to 4.32%, and the average SWI error was low to 0.95%. For individual subjects, the smallest SWI error was 0 on subject 10 and the largest SWI error was 4.32% on subject 15. The SWI estimation with an error less than 1%, 5%, and 10% accounted for 75% (15/20), 100% (20/20) and 100% (20/20) respectively on this dataset. Compared with the MA-EDM, the proposed individualized system significantly improved the overall SWI for these subjects, and achieved

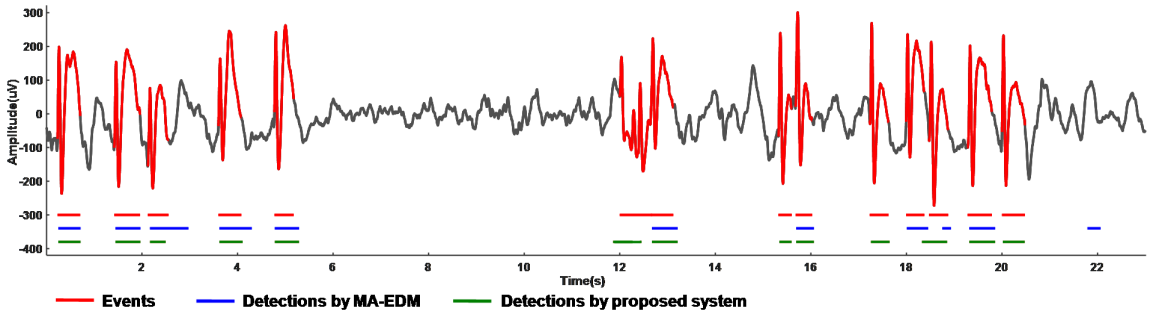

Fig. 6. Detection results of EEG series from the morphology analysis-based expert decision model with the traditional MA-EDM, and from that with automatic parameter setting-up (the proposed system), respectively. The red line denotes the events in the gold standard dataset. The detections from the two algorithms are denoted with blue and green lines, respectively. The starting and ending points of each line are the onset and offset of each event or detection.

TABLE I
SWI EVALUATION RESULTS OF 20 SUBJECTS ON THE SECOND DATASET

Subject	Sex	Age	SWI error (%)	
			MA-EDM [21]	Individualized system
1	Male	4	1.19	**0.46**
2	Male	11	**1.02**	3.38
3	Male	14	3.06	**0.34**
4	Male	9	3.27	**0.03**
5	Male	6	6.94	**2.10**
6	Male	8	4.50	**0.03**
7	Female	3	2.91	**0.25**
8	Female	8	1.89	**0.01**
9	Male	9	12.82	**0.51**
10	Female	7	1.60	**0.00**
11	Female	5	3.23	**0.05**
12	Male	5	5.30	**4.25**
13	Female	9	3.40	**0.24**
14	Male	10	1.54	**0.08**
15	Female	9	**1.16**	4.32
16	Male	13	7.50	**1.01**
17	Male	9	4.65	**0.51**
18	Male	4	3.24	**0.04**
19	Female	8	1.90	**0.95**
20	Female	6	4.36	**0.51**
Mean	/	8	3.77 (± 2.80)	**0.95** (± 1.41)

lower SWI error in most cases. For some subjects like subject 2 and 15, higher SWI errors were obtained by individualized system. It was mainly due to the fact that parameters in MA-EDM were manually adjusted for many trials over a long period of time. Meanwhile, for these subjects with higher SWI error, a relatively shorter recording was observed, which may indirectly affect the performance of the individualized system in parameter selection.

IV. DISCUSSION

This paper mimics the clinical decision-making process of ESES patterns by merging medical knowledge with signal morphology analysis. Meanwhile, the biogeography-based optimization technique is integrated into this morphology analysis-based expert decision model to form the hybrid expert system.

TABLE II
COMPARISON OF THE RESULTS ON THE FIRST DATASET FROM THE TRADITIONAL MA-EDM, AND FROM THAT WITH THE PROPOSED SYSTEM

	Algorithm	SWI error (%)
Group	MA-EDM matching	2.73
	Proposed generalized system	**1.49**
Subject A	MA-EDM matching	4.24
	Proposed individualized system	**0.62**
Subject B	MA-EDM matching	2.75
	Proposed individualized system	**0.86**
Subject C	MA-EDM matching	4.51
	Proposed individualized system	**0.64**
Subject D	MA-EDM matching	3.97
	Proposed individualized system	**0.49**

A. Performance Comparison Between Automatically Individualized Parameters and Manually Selected Parameters

We fully assess its results in terms of the detection and the percentage of spike and slow-waves during sleep. Fig. 6 displays the identification results of ESES patterns in EEG series from the system with manual parameter setting-up (the traditional MA-EDM), and with automatic parameter setting-up (the proposed system). Results before 6s show that the detections from the system with automatic parameters are closer to the actual events than those from the system with manual parameters. The detections from 12 to 13s and from 15 to 16s show that for such complex ESES patterns, the system with automatic parameters outperforms that with manual parameters. The identification results of ESES patterns in Fig. 6 show visually that the system with automatic parameter setting-up performs better, especially for the detection of complex spike and slow-waves.

Table II shows the comparison of the quantification results of ESES patterns. For all subjects, estimation errors in the SWI from the system with automatic parameters are significantly

less than those with manual parameters. The comparison results in Table II quantify the specific added-value of automatic parameter setting-up by the APS based on CMM-BBO as the initial step in the quantification process. Comparing the results for individuals and groups from Table II, the SWI error for the individuals ranges from 0.49% to 0.86% and the average SWI error of the group is 1.49%. The proposed system is able to obtain better results on different individuals and outperformed the generalized model, which illustrates the effectiveness of the individualized scheme.

Therefore, compared with predefined system parameters of manual regulation, the proposed individualized system of automatic parameter setting-up shows great capability for the quantification of EEG related to ESES.

B. Comparison Between Proposed Individualized ESES Quantification System and Existing Work

This study achieves the quantification of ESES by presenting a novel hybrid expert system. It is one of the few studies proposed for automatic ESES analysis in the literature [16], [18], [20]. We compare the presented individualized system with the existing relevant works for the detection and quantification of ESES activity. Evaluating EEG with the quantitative descriptor of ESES patterns, namely SWI, is the key to the diagnosis criteria [5]. Fig. 7 compares their performance on the first dataset from four subjects. Table III compares their performance by applying them to the same EEG recordings from a large population with ESES syndrome.

As shown in Fig. 7, our system obtained fewer errors in SWI estimation both on the group and individuals. Proposed system obtained the higher F1 scores on groups, but lower than that of the MA-EDM method for individual subjects, mainly due to the low proportion of training data. However, compared with MA-EDM, the feature extraction operation in our system was tailored to positive peaks and negative pits separately. Furthermore, we designed a BBO-based parameter selection procedure for the automatic setup of the system, which was more efficient than the manual setup in MA-EDM. After complementing it on partly data scored by the expert, the system was tuned by using optimal system parameters that had been adjusted to the data. Signal morphological variation and individualized differentiated features overlooked by the traditional MA-EDM were considered during our detection process.

Compared with template matching, K-mean clustering, and MA-EDM, the estimation error between the proposed system and the expert was 0.95%. The quantification performance of the proposed system was better than theirs both on the group and different subjects. Compared with the traditional MA-EDM, the SWI results from the proposed system were closer to that from the expert. As shown in Table III, the percentage of SWI error within 10% of the proposed systems was 100%. Compared with MA-EDM, the percentage of SWI errors within 1% was raised by the proposed system from 0 to 70%. MA-EDM relies on manual parameters, which is easy to fall into local optimization. Our proposed system can automatically set parameters to improve performance.

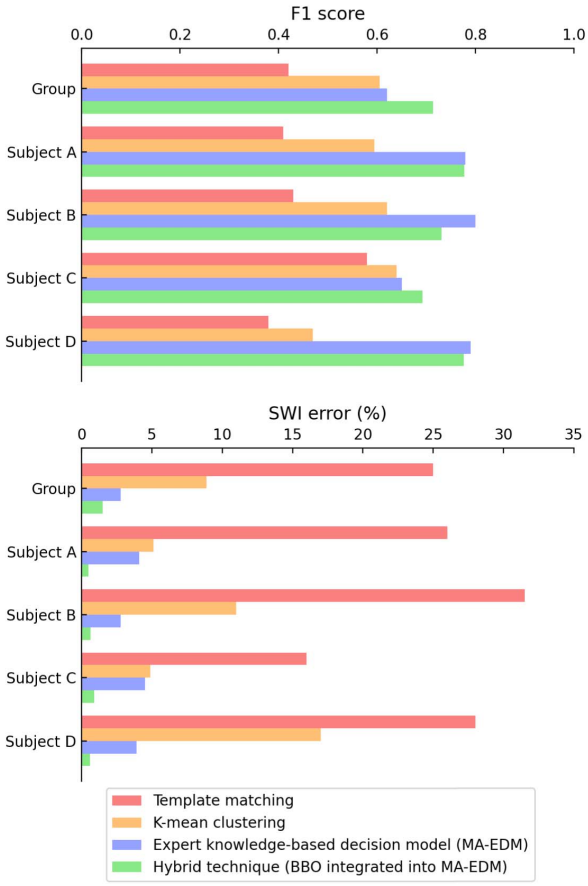

Fig. 7. Comparison with existing works for the quantification of ESES by performing them on the first database.

The clinical validation on the larger dataset indicates the ability of the presented system for the quantification of EEG related to ESES. From comparisons with existing methods in Fig. 7 and Table III, the overall performance of the proposed system was favorable and comparable.

Based on the limitations of the proposed system, we give a brief summary on the potential research. Firstly, more subjects should be involved to further enhance the method performance. With a limited dataset, we are dedicated to finding a minimum training data ratio that not only achieves fairly high accuracy, but also reduces the burden on the expert in labeling. This paper verifies the feasibility and reliability of the proposed system when only very small proportions of training data are available. Also, its performance can be improved when more training data are involved. The proposed method is conducted on a small dataset, which is accompanied by interpretability in combination with clinical analysis. However, further rigorous experiments with more data are required. In the future, we will collaborate with other hospitals/centers to collect more data to further verify the robustness of the proposed method. Secondly, multi-objective optimization algorithm should be considered. The result from Fig. 5 shows that the quantitative errors on the subjects could be relatively high due to the expanded recognition area where the algorithm aims to improve the F1 score. The quantitative errors on the subjects could be relatively high due to the expanded recognition area

TABLE III
COMPARISON WITH EXISTING WORKS FOR THE QUANTIFICATION OF ESES BY APPLYING THEM ON THE SECOND DATASET

Authors	Scheme	Detections of ESES pattern	SWI error (%)	The percentage of SWI error within		
				10%	5%	1%
A. Nonclercq et al.(2009) [16]	Template matching	Spike waves	2.95	75	40	15
A. Nonclercq et al.(2012) [18]	K-means clustering	Spike waves	2.14	80	50	10
Z. Xian et al. (2020) [21]	Knowledge-based decision model (MA-EDM)	Spike and slow-waves	3.77	95	80	0
Proposed individualized system	The hybrid technique (BBO integrated into MA-EDM)	Spike and slow-waves	**0.95**	**100**	**100**	**75**

where the algorithm aims to improve the F1 score. In our current approach, the single-objective optimization algorithm can only select one indicator for optimization. The development of multi-objective optimization algorithms is needed to achieve more accurate identification and lower estimation errors. The multi-objective optimization algorithm can increase the recognition precision and reduce the SWI estimation error in the meantime. The multi-objective optimization algorithm can increase the recognition precision and reduce the SWI estimation error in the meantime. Thirdly, clinical descriptions of ESES activity involve the topography and morphology of EEG. Multichannel analysis can be also researched by the proposed system to enhance its performance. Moreover, further explorations on the results obtained with our system may of significance for epilepsy research. At present, EEG is used to evaluate the SWI and has been used for the diagnosis of children's ESES, which plays an important role in clinical applications. Besides demonstrating the quantification results using SWI, it could be of clinical interest to explore various ESES patterns by classifying the detected spike and slow-waves.

V. CONCLUSION

This paper proposed a hybrid expert system for quantifying EEG related to electrical status epilepticus during sleep in children. It was constructed by integrating the biogeography-based optimization algorithm into a morphology analysis-based expert decision model. The morphology analysis-based expert decision model was designed by combining medical knowledge with signal morphology analysis. Then, to accomplish automatic optimization of the parameterized schemes for different features in the morphology analysis-based model, the biogeography-based optimization algorithm was applied to select optimal parameters for them by adjusting them in the decision-making process. As such, the expert decision model was tuned and performed using optimized schemes. In tuning the model, a more precise individualized framework that involves the personalized characteristics is proposed. With the exploration of the required amount of prior knowledge in selecting appropriate parameters, the proposed system can achieve an average SWI error of 0.95% by adopting only 10% of the individual data for generating the personalized parameters. Favorable results proved the ability and reliability of the presented system for quantifying ESES activity by considering both signal morphology and personalized characteristics. Meanwhile, the hybrid individualized expert system is expected to assist clinicians in precise ESES quantification analysis.

REFERENCES

[1] P. Gencpinar, N. Dundar, and H. Tekgul, "Electrical status epilepticus in sleep (ESES)/continuous spikes and waves during slow sleep (CSWS) syndrome in children: An electroclinical evaluation according to the EEG patterns," *Epilepsy Behav.*, vol. 61, pp. 107–111, Aug. 2016.

[2] I. S. Fernández, T. Loddenkemper, J. M. Peters, and S. V. Kothare, "Electrical status epilepticus in sleep: Clinical presentation and pathophysiology," *Pediatric Neurol.*, vol. 47, no. 6, pp. 390–410, Dec. 2012.

[3] S. Yilmaz, G. Serdaroglu, S. Gokben, and A. Akcay, "Clinical characteristics and outcome of children with electrical status epilepticus during slow wave sleep," *J. Pediatric Neurosci.*, vol. 9, no. 2, p. 105, 2014.

[4] Q. Yuan, F. Li, and H. Zhong, "Early diagnosis, treatment and prognosis of epilepsy with continuous spikes and waves during slow sleep," *Int. J. Clin. Exp. Med.*, vol. 8, no. 3, pp. 4052–4058, 2015.

[5] M. Scheltens-de-Boer, "Guidelines for EEG in encephalopathy related to ESES/CSWS in children," *Epilepsia*, vol. 50, pp. 13–17, Aug. 2009.

[6] I. S. Fernández, K. E. Chapman, J. M. Peters, C. Harini, A. Rotenberg, and T. Loddenkemper, "Continuous spikes and waves during sleep: Electroclinical presentation and suggestions for management," *Epilepsy Res. Treat.*, vol. 2013, pp. 1–12, Aug. 2013.

[7] N. Wiwattanadittakul, D. Depositario-Cabacar, and T. G. Zelleke, "Electrical status epilepticus in sleep (ESES)—Treatment pattern and EEG outcome in children with very high spike–wave index," *Epilepsy Behav.*, vol. 105, Apr. 2020, Art. no. 106965.

[8] D. Wang *et al.*, "Epileptic seizure detection in long-term EEG recordings by using wavelet-based directed transfer function," *IEEE Trans. Biomed. Eng.*, vol. 65, no. 11, pp. 2591–2599, Nov. 2018.

[9] I. Ullah, M. Hussain, E.-U.-H. Qazi, and H. Aboalsamh, "An automated system for epilepsy detection using EEG brain signals based on deep learning approach," *Exp. Syst. Appl.*, vol. 107, pp. 61–71, Oct. 2018.

[10] A. V. M. Misiūnas, T. Meškauskas, and R. Samaitienė, "Algorithm for automatic EEG classification according to the epilepsy type: Benign focal childhood epilepsy and structural focal epilepsy," *Biomed. Signal Process. Control*, vol. 48, pp. 118–127, Feb. 2019.

[11] K. M. Tsiouris, V. C. Pezoulas, M. Zervakis, S. Konitsiotis, D. D. Koutsouris, and D. I. Fotiadis, "A long short-term memory deep learning network for the prediction of epileptic seizures using EEG signals," *Comput. Biol. Med.*, vol. 99, pp. 24–37, Aug. 2018.

[12] C. Chen, A. Ugon, C. Sun, W. Chen, C. Philippe, and A. Pinna, "Towards a hybrid expert system based on sleep event's threshold dependencies for automated personalized sleep staging by combining symbolic fusion and differential evolution algorithm," *IEEE Access*, vol. 7, pp. 1775–1792, 2019.

[13] S. Supriya, S. Siuly, H. Wang, and Y. Zhang, "Epilepsy detection from EEG using complex network techniques: A review," *IEEE Rev. Biomed. Eng.*, early access, Feb. 1, 2021, doi: 10.1109/RBME.2021.3055956.

[14] S. Supriya, S. Siuly, H. Wang, and Y. Zhang, "New feature extraction for automated detection of epileptic seizure using complex network framework," *Appl. Acoust.*, vol. 180, Sep. 2021, Art. no. 108098.

[15] R. Zarei, J. He, S. Siuly, G. Huang, and Y. Zhang, "Exploring Douglas–Peucker algorithm in the detection of epileptic seizure from multicategory EEG signals," *BioMed Res. Int.*, vol. 2019, Jul. 2019, Art. no. 5173589.

[16] A. Nonclercq *et al.*, "Spike detection algorithm automatically adapted to individual patients applied to spike and wave percentage quantification," *Neurophysiol. Clinique/Clin. Neurophysiol.*, vol. 39, pp. 123–131, Apr. 2009.

[17] C. A. Tassinari, G. Cantalupo, L. Rios-Pohl, E. D. Giustina, and G. Rubboli, "Encephalopathy with status epilepticus during slow sleep: "The Penelope syndrome," *Epilepsia*, vol. 50, pp. 4–8, Aug. 2009.

[18] A. Nonclercq *et al.*, "Cluster-based spike detection algorithm adapts to interpatient and intrapatient variation in spike morphology," *J. Neurosci. Methods*, vol. 210, no. 2, pp. 259–265, Sep. 2012.

[19] F. E. Abd El-Samie, T. N. Alotaiby, M. I. Khalid, S. A. Alshebeili, and S. A. Aldosari, "A review of EEG and MEG epileptic spike detection algorithms," *IEEE Access*, vol. 6, pp. 60673–60688, 2018.

[20] T. Fukami, T. Shimada, and B. Ishikawa, "Fast EEG spike detection via eigenvalue analysis and clustering of spatial amplitude distribution," *J. Neural Eng.*, vol. 15, no. 3, Jun. 2018, Art. no. 036030.

[21] X. Zhao *et al.*, "A knowledge-based approach for automatic quantification of epileptiform activity in children with electrical status epilepticus during sleep," *J. Neural Eng.*, vol. 17, no. 4, Aug. 2020, Art. no. 046032.

[22] C. Iber, S. Ancoli-Israel, A. Chesson, and S. Quan, "The AASM manual for the scoring of sleep and associated events: Rules, terminology and technical specifications," *Westchester, IL, Amer. Acad. Sleep Med.*, Jan. 2007.

[23] C.-H. H. Chu and E. J. Delp, "Impulsive noise suppression and background normalization of electrocardiogram signals using morphological operators," *IEEE Trans. Biomed. Eng.*, vol. 36, no. 2, pp. 262–273, Feb. 1989.

[24] B. Krishnan *et al.*, "A novel spatiotemporal analysis of peri-ictal spiking to probe the relation of spikes and seizures in epilepsy," *Ann. Biomed. Eng.*, vol. 42, no. 8, pp. 1606–1617, Aug. 2014.

[25] S. Al-Sharhan and A. Bimba, "Adaptive multi-parent crossover GA for feature optimization in epileptic seizure identification," *Appl. Soft Comput.*, vol. 75, pp. 575–587, Feb. 2019.

[26] A. De, J. Wang, and M. K. Tiwari, "Hybridizing basic variable neighborhood search with particle swarm optimization for solving sustainable ship routing and bunker management problem," *IEEE Trans. Intell. Transp. Syst.*, vol. 21, no. 3, pp. 986–997, Mar. 2020.

[27] C. Darwin and J. Huxley, *The Origin of Species: 150th Anniversary Edition*, 150th ed. New York, NY, USA: Signet, Sep. 2003.

[28] A. R. Wallace, *The Geographical Distribution of Animals: With a Study of the Relations of Living and Extinct Faunas as Elucidating the Past Changes of the Earth's Surface*. Prague, Czech Republic: E-artnow, Aug. 2020.

[29] R. H. MacArthur and E. O. Wilson, *The Theory of Island Biogeography*. Princeton, NJ, USA: Princeton Univ. Press, Apr. 2001.

[30] R. Dhiman, J. S. Saini, and Priyanka, "Biogeography based hybrid scheme for automatic detection of epileptic seizures from EEG signatures," *Appl. Soft Comput.*, vol. 51, pp. 116–129, Feb. 2017.

[31] K. Liu, C. Zou, K. Li, and T. Wik, "Charging pattern optimization for lithium-ion batteries with an electrothermal-aging model," *IEEE Trans. Ind. Informat.*, vol. 14, no. 12, pp. 5463–5474, Dec. 2018.

[32] A. R. Kashani, M. Gandomi, C. V. Camp, and A. H. Gandomi, "Optimum design of shallow foundation using evolutionary algorithms," *Soft Comput.*, vol. 24, no. 9, pp. 6809–6833, May 2020.

[33] D. Simon, "Biogeography-based optimization," *IEEE Trans. Evol. Comput.*, vol. 12, no. 6, pp. 702–713, Dec. 2008.

[34] D. Simon, M. G. H. Omran, and M. Clerc, "Linearized biogeography-based optimization with re-initialization and local search," *Inf. Sci.*, vol. 267, pp. 140–157, May 2014.

[35] G. Xiong, D. Shi, and X. Duan, "Enhancing the performance of biogeography-based optimization using polyphyletic migration operator and orthogonal learning," *Comput. Oper. Res.*, vol. 41, pp. 125–139, Jan. 2014.

[36] P. Savsani, R. L. Jhala, and V. Savsani, "Effect of hybridizing biogeography-based optimization (BBO) technique with artificial immune algorithm (AIA) and ant colony optimization (ACO)," *Appl. Soft Comput.*, vol. 21, pp. 542–553, Aug. 2014.

[37] W. Gong, Z. Cai, and C. X. Ling, "DE/BBO: A hybrid differential evolution with biogeography-based optimization for global numerical optimization," *Soft Comput.*, vol. 15, no. 4, pp. 645–665, Apr. 2010.

[38] X.-W. Zheng, D.-J. Lu, X.-G. Wang, and H. Liu, "A cooperative coevolutionary biogeography-based optimizer," *Appl. Intell.*, vol. 43, no. 1, pp. 95–111, 2015.

[39] X. Chen, H. Tianfield, W. Du, and G. Liu, "Biogeography-based optimization with covariance matrix based migration," *Appl. Soft Comput.*, vol. 45, pp. 71–85, Aug. 2016.

[40] W. Gong, Z. Cai, C. X. Ling, and H. Li, "A real-coded biogeography-based optimization with mutation," *Appl. Math. Comput.*, vol. 216, no. 9, pp. 2749–2758, Jul. 2010.

[41] S. C. Warby *et al.*, "Sleep–spindle detection: Crowdsourcing and evaluating performance of experts, non–experts and automated methods," *Nature Methods*, vol. 11, pp. 385–392, Apr. 2014.

[42] J. Redmon, S. Divvala, R. Girshick, and A. Farhadi, "You only look once: Unified, real-time object detection," in *Proc. IEEE Conf. Comput. Vis. Pattern Recognit. (CVPR)*, Las Vegas, NV, USA, June 2016, pp. 779–788.

[43] S. Chambon, V. Thorey, P. J. Arnal, E. Mignot, and A. Gramfort, "DOSED: A deep learning approach to detect multiple sleep micro-events in EEG signal," *J. Neurosci. Methods*, vol. 321, pp. 64–78, Jun. 2019.